

# *Assessing the performance of data assimilation algorithms which employ linear error feedback*

Article

Accepted Version

Mallia-Parfitt, N. and Bröcker, J. (2016) Assessing the performance of data assimilation algorithms which employ linear error feedback. *Chaos*, 26 (10). 103109. ISSN 1089-7682 doi: 10.1063/1.4965029 Available at <https://centaur.reading.ac.uk/67574/>

It is advisable to refer to the publisher's version if you intend to cite from the work. See [Guidance on citing](#).

To link to this article DOI: <http://dx.doi.org/10.1063/1.4965029>

Publisher: American Institute of Physics

All outputs in CentAUR are protected by Intellectual Property Rights law, including copyright law. Copyright and IPR is retained by the creators or other copyright holders. Terms and conditions for use of this material are defined in the [End User Agreement](#).

[www.reading.ac.uk/centaur](http://www.reading.ac.uk/centaur)



<sup>1</sup> **Assessing the Performance of Data Assimilation Algorithms which employ Linear  
2 Error Feedback**

<sup>3</sup> Noeleene Mallia-Parfitt<sup>1</sup> and Jochen Bröcker<sup>1</sup>

<sup>4</sup> *School of Mathematical, Physical and Computational Sciences,*

<sup>5</sup> *University of Reading, Whiteknights, PO BOX 220, Reading, RG6 6AX,*

<sup>6</sup> *United Kingdom*

<sup>7</sup> (Dated: 4 October 2016)

Data assimilation means to find an (approximate) trajectory of a dynamical model that (approximately) matches a given set of observations. A direct evaluation of the trajectory against the available observations is likely to yield a too optimistic view of performance, since the observations were already used to find the solution. A possible remedy is presented which simply consists of estimating that optimism, thereby giving a more realistic picture of the ‘out of sample’ performance. Our approach is inspired by methods from statistical learning employed for model selection and assessment purposes in statistics. Applying similar ideas to data assimilation algorithms yields an operationally viable means of assessment. The approach can be used to improve the performance of models or the data assimilation itself. This is illustrated by optimising the feedback gain for data assimilation employing linear feedback.

<sup>8</sup> Data assimilation means to find an (approximate) trajectory of a dynamical  
<sup>9</sup> model that (approximately) matches a given set of observations. A fundamental  
<sup>10</sup> problem of data assimilation experiments in atmospheric contexts is that there  
<sup>11</sup> is no possibility of replication, that is, truly “out of sample” observations from  
<sup>12</sup> the same underlying flow pattern but with independent observational errors are  
<sup>13</sup> typically not available. A direct evaluation against the available observations  
<sup>14</sup> is likely to yield unrealistic results though, since the observations were already  
<sup>15</sup> used to find the solution. A possible remedy is presented which simply consists  
<sup>16</sup> of estimating that optimism, thereby giving a more realistic picture of the ‘out of  
<sup>17</sup> sample’ performance. The approach is particularly simple when applied to data  
<sup>18</sup> assimilation algorithms employing linear error feedback. A realistic performance  
<sup>19</sup> assessment is obtained by comparing with the true trajectory. In addition this  
<sup>20</sup> method provides a simple and efficient means to determine the optimal feedback  
<sup>21</sup> gain operationally since it only requires known quantities to be calculated. The  
<sup>22</sup> optimality of this gain is verified numerically. Further, we illustrate theoretical  
<sup>23</sup> results which demonstrate that in linear systems with gaussian perturbations,  
<sup>24</sup> the feedback thus determined will approach the optimal (Kalman) gain in the  
<sup>25</sup> limit of large observational windows (the proof will be given elsewhere).

---

## <sup>26</sup> I. INTRODUCTION

<sup>27</sup> Data Assimilation involves the incorporation of observational data into a numerical model  
<sup>28</sup> to produce a model state that accurately describes the observed reality. This procedure  
<sup>29</sup> uses an explicit dynamical model for the time evolution of the observed reality. The results  
<sup>30</sup> produced by data assimilation must satisfy two requirements. Firstly they must be close to  
<sup>31</sup> the observations up to a certain degree of accuracy and secondly they should be consistent  
<sup>32</sup> with the dynamical model to a certain degree of accuracy. In other words, the trajectory  
<sup>33</sup> produced by data assimilation must be close to the observations and it must be close to  
<sup>34</sup> being an orbit of the model.

<sup>35</sup> Once the observations have been used to estimate these trajectories, they should not be  
<sup>36</sup> used to evaluate the performance of the model (at least not without precaution) as this

<sup>37</sup> might give unrealistic results. Simply comparing the observations with the output of the  
<sup>38</sup> data assimilation scheme will provide an overly optimistic picture of performance. Moreover,  
<sup>39</sup> assessing the performance using this tracking error could easily be cheated. An example is  
<sup>40</sup> taking the output to be the observations themselves.

<sup>41</sup> As we will see in Section II, a more realistic evaluation of the performance needs to take  
<sup>42</sup> into account that the output and the observation errors are correlated. To this end, we  
<sup>43</sup> investigate the concept of out-of-sample error from statistics and adapt it to the problem of  
<sup>44</sup> data assimilation. In statistics, estimates of the out-of-sample error are used to measure how  
<sup>45</sup> well a statistical model, after fitting it to observations, generalises to unseen data<sup>1,2</sup>. Although  
<sup>46</sup> the concept of the out-of-sample error is a very general one, actual implementations differ  
<sup>47</sup> considerably depending on the structure of the estimation problem. Further, a fundamental  
<sup>48</sup> assumption often made in statistics is that the observations (conditionally on the explanatory  
<sup>49</sup> variables) are independent and identically distributed. In the case of linear regression models,  
<sup>50</sup> a popular statistic for model selection in statistical learning is the Cp statistic<sup>3,4</sup>. Other  
<sup>51</sup> examples are Akaike's Information Criterion (AIC) or the Bayesian Information Criterion  
<sup>52</sup> (BIC). These concepts differ in terms of precise interpretation and range of applicability.

<sup>53</sup> The aim of this paper is to provide similar tools in the context of data assimilation.  
<sup>54</sup> The underlying problem is essentially the same as in statistics. Suppose a time series of  
<sup>55</sup> observations has been assimilated into a dynamical model. Then the output should be close  
<sup>56</sup> to hypothetical observations from the same flow patterns but with independent errors. If  
<sup>57</sup> the results are not close to these hypothetical observations, then this can only mean that  
<sup>58</sup> the model is in fact not able to explain the dynamics underlying the observations. The  
<sup>59</sup> out-of-sample error should be a measure of how close the output will be to such hypothetical  
<sup>60</sup> observations. Although observations from the same flow pattern but with independent errors  
<sup>61</sup> are typically not available in practice, we show that the out-of-sample error can be estimated  
<sup>62</sup> using terms that are operationally available. Specifically we show that the out-of-sample  
<sup>63</sup> error is the sum of the tracking error and a term which we call the optimism. This optimism  
<sup>64</sup> gives us a representation of how the model and observations depend on each other and it  
<sup>65</sup> quantifies how much the tracking error misestimates the out-of-sample error. The derived  
<sup>66</sup> expression is reminiscent of the Cp statistic used in model selection in statistical learning<sup>3,4</sup>.  
<sup>67</sup> We show that the optimism takes a very simple form if we assume that the model employs a  
<sup>68</sup> linear error feedback. There are many data assimilation algorithms that implement such a

<sup>69</sup> feedback<sup>5</sup>. More details and references concerning such algorithms can be found in section II.

<sup>70</sup> Wahba *et al.*<sup>6</sup> apply the ideas of out-of-sample performance to data assimilation for linear  
<sup>71</sup> systems. In this publication they use generalised cross validation to get an estimate of the  
<sup>72</sup> true performance. The key equation in this paper is equation (2.11) which is similar to  
<sup>73</sup> equation (7.46) in Hastie, Tibshirani, and Friedman<sup>3</sup> with the new aspect being the stochastic  
<sup>74</sup> approximation to the denominator. The results presented in Wahba *et al.*<sup>6</sup> however, apply  
<sup>75</sup> only in a linear context. As it will be shown, the analysis presented in our paper does not  
<sup>76</sup> require linear models but merely linear error feedback.

<sup>77</sup> We stress that although in terms of the problem we are addressing there is a strong  
<sup>78</sup> similarity between statistics and data assimilation, our analysis will be different. For instance,  
<sup>79</sup> although the data assimilation uses linear error feedback, the dependence of the output  
<sup>80</sup> on the observations as a whole is nonlinear, due to the nonlinearity of the dynamic model.  
<sup>81</sup> Further, the observations are not independent. The derivation of the Cp statistic, AIC,  
<sup>82</sup> BIC and many other related concepts used in statistics however assumes either linearity,  
<sup>83</sup> independence or both (see Hastie, Tibshirani, and Friedman<sup>3</sup>, Sec 7.4).

<sup>84</sup> We demonstrate the usefulness of our approach with three numerical examples. In all  
<sup>85</sup> three cases, we consider a simple data assimilation scheme by means of filtering with a  
<sup>86</sup> linear error feedback. A persistent problem in practice is to find a suitable feedback. The  
<sup>87</sup> feedback acts as a coupling between the true dynamics and the model. If the coupling is too  
<sup>88</sup> weak the stability of the system cannot be guaranteed while if the coupling is too strong,  
<sup>89</sup> results deteriorate because the noise will be overly attenuated. Striking the right balance  
<sup>90</sup> requires a reliable assessment of the performance which is provided by our estimate of the  
<sup>91</sup> out-of-sample performance. Note that this is relevant even in the case of linear systems  
<sup>92</sup> with gaussian perturbations as computing the theoretically optimal Kalman Gain requires  
<sup>93</sup> knowledge of the dynamical noise which is usually not available in practice. Our experiments  
<sup>94</sup> demonstrate that the technique can be used in situations where the feedback gain matrix is  
<sup>95</sup> completely unspecified and also in situations where it has a pre-determined structure but  
<sup>96</sup> contains unknown parameters.

<sup>97</sup> In section II we define the tracking error, out-of-sample error and the optimism. These  
<sup>98</sup> considerations are valid for any data assimilation algorithm in the case of additive observa-  
<sup>99</sup> tional noise. We also consider general data assimilation algorithms which employ linear error  
<sup>100</sup> feedback and determine an analytical expression for the optimism. Section III contains several

101 numerical experiments. In Section III A we apply the methodology to a linear system with  
 102 gaussian perturbations. We minimise an estimate of the out-of-sample error to determine a  
 103 feedback gain. We then compare this with the asymptotic Kalman Gain which is known to  
 104 be optimal in this situation. Our experiments suggest that the gain determined numerically  
 105 agrees with the optimal Kalman Gain in the limit of large observation windows. We discuss a  
 106 theoretical result which confirms this finding. Next we consider a situation in which the data  
 107 assimilation algorithm is constrained to have poles in certain locations which determines the  
 108 gain up to a single parameter. This parameter is determined by minimising an estimate of  
 109 the out-of-sample error.

110 The remaining experiments consider non linear systems. In Section III B we consider  
 111 a system in Lur'e form. These systems are special in that, despite being non linear, they  
 112 permit observers with linear error dynamics. Again a linear feedback is used and we show  
 113 how an estimate of the out-of-sample error can be used to determine the feedback. The  
 114 performance of this feedback is assessed numerically by considering the error between the  
 115 reconstructed and the true orbit. Our results indicate that this strategy of choosing the  
 116 feedback gives close to optimal performance. Repeating the experiment with the Lorenz '96  
 117 system in Section III C confirm the results.

## 118 **II. TRACKING ERROR, OUTPUT ERROR AND OPTIMISM IN DATA 119 ASSIMILATION**

120 Data assimilation is the procedure by which trajectories  $\{z_n \in \mathbb{R}^D, n = 1, \dots, N\}$  (in some  
 121 state space which we take to be  $\mathbb{R}^D$ ) are computed with the help of a dynamical model and  
 122 observations,  $\{\eta_n, n = 1, \dots, N\}$ . These trajectories should reproduce the observations up to  
 123 some degree of accuracy for all  $n = 1, \dots, N$ . We express this latter part of the procedure  
 124 formally as: The output  $y_n = h(z_n)$  is close to the observations  $\{\eta_n, n = 1, \dots, N\}$  up to  
 125 some degree of accuracy, where  $h : \mathbb{R}^D \rightarrow \mathbb{R}^d$  is a function which maps the model's state  
 126 space into the observation space. This function is usually part of the problem specification.  
 127 The exact structure of the model and of  $h$  is not important at this stage.

128 Suppose we have observations  $\{\eta_n \in \mathbb{R}^d, n = 1, \dots, N\}$  from some real world dynamical  
 129 phenomenon. We assume  $\eta_n$  can be written as

$$\eta_n = \zeta_n + \sigma r_n \quad (1)$$

130 where  $\{\zeta_n, n = 1, \dots, N\}$  are unknown quantities representing the desired signal, and  $\sigma \in$   
 131  $\mathbb{R}^{d \times d}$  is the observational error standard deviation. We assume that  $\{\zeta_n, n = 1, \dots, N\}$  can  
 132 be modelled as some stochastic process. The observation errors or noise,  $\{r_n, n = 1, \dots, N\}$   
 133 are assumed to be independent with mean  $\mathbb{E}r_n = 0$  and variance  $\mathbb{E}r_n r_n^T = \mathbb{I}$  and they are  
 134 independent of  $\{\zeta_n, n = 1, \dots, N\}$ .

135 Deviation of the output from the observations can be quantified by means of the tracking  
 136 error,

$$E_T = \mathbb{E}[y_n - \eta_n]^2. \quad (2)$$

137 The tracking error though is not a very useful performance measure of data assimilation  
 138 approaches. It is not difficult to design algorithms which achieve zero tracking error by  
 139 simply using the observations as output, that is any DA algorithm which satisfies  $y_n = \eta_n$ ,  
 140  $n = 1, \dots, N$  achieves optimal performance with respect to  $E_T$  as a performance measure.

141 A performance measure which is much harder to hedge is the output error

$$E_O = \mathbb{E}[y_n - \zeta_n]^2. \quad (3)$$

142 A useful relation between  $E_O$  and  $E_T$  can be established. Substituting the expression (1) for  
 143 the observations into (2) and expanding, we get

$$E_T = \mathbb{E}[y_n - \eta_n]^2 = \mathbb{E}[y_n - \zeta_n]^2 + \text{tr}(\sigma^T \sigma) - 2\text{tr}(\sigma \mathbb{E}[r_n y_n^T]) \quad (4)$$

144 since  $\zeta_n$  and  $r_n$  are independent. The notation 'tr' denotes the trace of the matrix.

145 We re-write this as

$$E_O + \text{tr}(\sigma^T \sigma) = \mathbb{E}[y_n - \eta_n]^2 + 2\text{tr}(\sigma \mathbb{E}[r_n y_n^T]). \quad (5)$$

146 The term  $2\sigma \mathbb{E}[r_n y_n^T]$  is called the *optimism*. The optimism should be understood as a  
 147 correlation between  $r_n$  and  $y_n$ , where  $y_n$  depends on  $\{r_k, k = 1, \dots, N\}$ . It is a measure  
 148 of how much the tracking error misestimates the output error. We will argue that both  
 149 the optimism and the tracking error (i.e the first term on the right hand side of (5) can  
 150 be estimated using operationally available quantities. This will give us a handle on the  
 151 output error which is, as we have argued, directly related to the true performance of the  
 152 data assimilation.

153 The quantity  $E_O + \sigma^2$  can be interpreted as an "Out-of-sample error" as follows: Define  
 154 hypothetical observations

$$\eta'_n = \zeta_n + r'_n, \quad n = 1, \dots, N \quad (6)$$

155 where  $\{\zeta_n, n = 1, \dots, N\}$  is as before,  $\{r'_n, n = 1, \dots, N\}$  is a process with the same  
 156 distribution as  $\{r_n, n = 1, \dots, N\}$  but independent from it. Then the out-of-sample error is  
 157 the error between  $\{y_n, n = 1, \dots, N\}$  and  $\{\eta'_n, n = 1, \dots, N\}$ , which can be written as

$$\mathbb{E}[y_n - \eta'_n]^2 = E_O + \sigma^2. \quad (7)$$

158 The key difference between the tracking error and the out-of-sample error is the absence of  
 159 correlation between  $\{y_n, n = 1, \dots, N\}$  and  $\{r'_n, n = 1, \dots, N\}$  in the latter, which is precisely  
 160 the optimism.

161 Equation (5) shows that the tracking error augmented with further terms, can be a useful  
 162 measure of performance. Further the tracking error and optimism are relatively easy to  
 163 estimate. In our experiments we will estimate the tracking error through an empirical average,  
 164 namely

$$\hat{E}_T = \frac{1}{N} \sum_{k=1}^N (y_k - \eta_k)^2. \quad (8)$$

165 Estimates of the optimism will be discussed next.

166 We will first calculate a general expression for the optimism for data assimilation schemes  
 167 which employ a linear error feedback. Most operational data assimilation schemes work in  
 168 cycles over time. The *background field*,  $\hat{z}_n$ , is computed at the start of each cycle and usually  
 169 it is based on information from previous cycles. Since any cycle uses observations available  
 170 up to that point, the background field at time  $n$  only depends on  $\eta_1, \dots, \eta_{n-1}$ . Nonetheless,  
 171 the background field  $\hat{z}_n$  is supposed to be a first guess of the the state of the system at time  
 172  $n$ .

173 In this paper we consider data assimilation algorithms which combine the new observation  
 174 and background through a relationship of the form

$$z_n = \hat{z}_n + \mathbf{K}_n(\eta_n - h(\hat{z}_n)) \quad (9)$$

175 where  $\mathbf{K}_n$  is a  $D \times d$  matrix and can depend on  $\eta_1, \dots, \eta_{n-1}$  but not on  $\eta_n$ . As before, the  
 176 mapping  $h : \mathbb{R}^D \rightarrow \mathbb{R}^d$ , maps points from model state space to observation space. The  
 177 modified background,  $z_n$ , is referred to as the *analysis*.

178 The matrix  $\mathbf{K}_n$  is the error feedback gain. Equation (9) tells us that the analysis has a  
 179 linear dependence on the current observation,  $\eta_n$  and it depends on the previous observations  
 180 through  $\mathbf{K}_n$  and  $\hat{z}_n$ . Data assimilation schemes that fall into the presented approach include

<sup>181</sup> Successive Correction Method (SCM)<sup>7,8</sup>; Optimal Interpolation (OI)<sup>9</sup>; 3D-Var<sup>10,11</sup>; Kalman  
<sup>182</sup> Filter variants,<sup>12</sup> and certain Synchronisation approaches. Synchronisation between dynamical  
<sup>183</sup> systems has been studied for some time, see for example Pikovsky, Rosenblum, and Kurths<sup>13</sup>;  
<sup>184</sup> Huijberts, Nijmeijer, and Pogromsky<sup>14</sup>; Boccaletti *et al.*<sup>15</sup>. Synchronisation in the setting of  
<sup>185</sup> data assimilation has also been studied, see Bröcker and Szendro<sup>16</sup>; Szendro, Rodríguez, and  
<sup>186</sup> Lopez<sup>17</sup>; Yang, Baker, and Li<sup>18</sup>. These methods differ only on the approach they take to  
<sup>187</sup> calculate the background  $\hat{z}_n$  and the matrix  $\mathbf{K}_n$ <sup>5</sup>.

We now consider the optimism as in (5) in the context of DA scheme with linear feedback as in (9). We assume that the function  $h(x_n)$  is linear so that  $h(x_n) = \mathbf{H}x_n$ , where  $\mathbf{H}$  is a  $d \times D$  matrix. Then,

$$\mathbb{E}[r_n y_n^T] = \mathbb{E}[r_n(\mathbf{H}z_n)^T] = \mathbb{E}[r_n z_n^T] \mathbf{H}^T \quad (10)$$

$$= \mathbb{E}[r_n \{(\mathbb{1} - \mathbf{K}_n \mathbf{H}) \hat{z}_n + \mathbf{K}_n(\zeta_n + \sigma r_n)\}^T] \mathbf{H}^T \quad (11)$$

$$\begin{aligned} &= \mathbb{E}[r_n ((\mathbb{1} - \mathbf{K}_n \mathbf{H}) \hat{z}_n)^T] \mathbf{H}^T \\ &\quad + \mathbb{E}[r_n (\mathbf{K}_n \zeta_n)^T] \mathbf{H}^T + \mathbb{E}[r_n (\mathbf{H} \mathbf{K}_n \sigma r_n)^T] \end{aligned} \quad (12)$$

$$= \mathbb{E}[r_n r_n^T \sigma^T \mathbf{K}_n^T] \mathbf{H}^T \quad (13)$$

$$= \text{tr}(\mathbb{E}[r_n r_n^T] \sigma^T \bar{\mathbf{K}}_n^T \mathbf{H}^T) \quad (14)$$

<sup>188</sup> where  $\bar{\mathbf{K}}_n = \mathbb{E}[\mathbf{K}_n]$ . The first two equalities, (10) and (11), are obtained by substituting the  
<sup>189</sup> relevant information while (12) is obtained by simply expanding the previous equation. The  
<sup>190</sup> derivation from (12) to (13) requires some explanation. Notice first that only the third term  
<sup>191</sup> of (12) survives. The first term is equal to zero because  $\hat{z}_n$  and  $\mathbf{K}_n$  are uncorrelated with  
<sup>192</sup>  $r_n$ . The second term is also equal to zero because  $\zeta_n$  is independent of  $r_n$  and because the  
<sup>193</sup> coupling matrix  $\mathbf{K}_n$  depends on the observations  $(\eta_1 \dots \eta_{n-1})$  and thus is uncorrelated with  
<sup>194</sup>  $r_n$ .

<sup>195</sup> Therefore, we are only left with the third term of (12) in (13). Since  $\mathbb{E}(r_n r_n^T) = \mathbb{1}$ , (14)  
<sup>196</sup> implies that

$$2\text{tr}(\sigma \mathbb{E}[r_n y_n^T]) = 2\text{tr}(\sigma \cdot \sigma^T \bar{\mathbf{K}}_n^T \mathbf{H}^T). \quad (15)$$

<sup>197</sup> In the case when  $d = 1$ , which is the case we consider in the numerical experiments later,  
<sup>198</sup> this reduces to

$$2\sigma \mathbb{E}[y_n r_n] = 2\mathbf{H} \bar{\mathbf{K}}_n \sigma^2. \quad (16)$$

199 We recall that the assumptions necessary to derive this formula are a linear observation  
200 operator,  $r_n$  is independent of  $\{\eta_1, \dots, \eta_{n-1}\}$ ,  $\mathbb{E}r_n = 0$ ,  $\mathbb{E}r_n r_n^T = \mathbb{1}$  and  $\mathbf{K}_n$  depends only on  
201 the observations  $(\eta_1, \dots, \eta_{n-1})$ .

202 In our numerical experiments we approximate the expected value of a random variable by  
203 the empirical mean. In particular  $E_T$  is replaced by its empirical average in (5), resulting in  
204 the following estimate for  $E_O$  for all subsequent numerical experiments (in which  $\mathbf{K}_n$  is in  
205 fact constant):

$$\hat{E}_O = \hat{E}_T + \frac{1}{N} \sum_{n=1}^N 2\sigma^2 \text{tr}(\bar{\mathbf{K}}_n^T \mathbf{H}^T) - \sigma^2. \quad (17)$$

206 Let us briefly digress on how the background  $\hat{z}_n$  and  $\mathbf{K}_n$  might be calculated in the context  
207 of synchronisation, although this is in fact irrelevant for the optimism. Suppose that the  
208 reality is given by the non linear dynamical system

$$\begin{aligned} x_{n+1} &= \tilde{f}(x_n) \\ \zeta_n &= \tilde{h}(x_n) \\ \eta_n &= \zeta_n + \sigma r_n \end{aligned} \quad (18)$$

209 where  $x_n \in \mathbb{R}^D$  is referred to as the state and  $\zeta_n \in \mathbb{R}^d$  are the true observations. For this  
210 non linear dynamical system we construct a sequential scheme

$$\begin{aligned} \hat{z}_{n+1} &= f(z_n) \\ z_{n+1} &= \hat{z}_{n+1} - \mathbf{K}_n(h(\hat{z}_{n+1}) - \eta_{n+1}) \\ y_n &= h(z_n) \end{aligned} \quad (19)$$

211 where  $\mathbf{K}_n$  is a  $D \times d$  coupling matrix which depends on the observations  $\eta_1, \dots, \eta_n$  but  
212 not on  $\eta_{n+1}$ ; and  $y_n$  is the model output where we hope that  $y_n \cong \zeta_n$ . Here  $f$  and  $h$  are  
213 approximations to the functions  $\tilde{f}$  and  $\tilde{h}$ , respectively. The coupling introduced in this  
214 scheme creates a linear feedback, in the sense that the error between  $y_n = h(\hat{z}_n)$  and the  
215 observations  $\eta_n$  is fed back into the model.

216 Synchronisation refers to a situation in which, due to coupling, the error  $y_n - \eta_n$  becomes  
217 small asymptotically irrespective of the initial conditions for the model<sup>13</sup>. Often a control  
218 theoretic approach is taken to determine conditions which guarantee the model output,  
219  $y_n = h(z_n)$ , converging to the observations,  $\eta_n$  or even  $z_n$  converging to  $x_n$  (strictly speaking,  
220 the difference converging to zero; note that this can only be expected in case of noise free  
221 observations).

222 It has been highlighted above that the tracking error is not an ideal measure of performance;  
 223 however the output error is and moreover, it can be calculated using terms that are readily  
 224 available. An important question that arises in operational practice is to how to choose  
 225 the gain matrix  $\mathbf{K}$ . The numerical experiments detailed below consider different conditions  
 226 under which to select the appropriate coupling matrix to use in the assimilation. For the  
 227 first linear experiment we consider arbitrary candidates for the gain matrix, while for the  
 228 second linear experiment we consider gains that guarantee a certain structure of the system  
 229 matrix (or more specifically the poles thereof).

### 230 III. NUMERICAL EXPERIMENTS

231 We now demonstrate the usefulness of our approach with three numerical examples. In  
 232 Section III A we present the methodology for a linear system with gaussian perturbations. We  
 233 minimise an estimate of the out-of-sample error to determine a feedback gain and compare  
 234 this with the asymptotic Kalman Gain which is known to be optimal in this situation.

235 The remaining two experiments concern nonlinear systems. In Section III B we present  
 236 numerical results for the Hénon Map and in Section III C results are established for the  
 237 Lorenz'96 System. Again a linear feedback is used and we show how an estimate of the  
 238 out-of-sample error can be used to determine the feedback.

239 There is some repetition in the obtained results, however this repetition validates our  
 240 approach across different experiments. The three systems we consider all use a data assimi-  
 241 lation scheme that employs linear error feedback. However the underlying systems in each  
 242 are different; one is linear, one is in Lur'e form and one is nonlinear. The similarities in the  
 243 results confirm that our methodology applies to many different dynamical systems.

#### 244 A. Numerical Experiment 1: Linear Map

245 In this first linear example the following experimental setup was used: The reality is given  
 246 by

$$x_{n+1} = \underbrace{\begin{bmatrix} -1 & 10 \\ 0 & 0.5 \end{bmatrix}}_A x_n + \rho q_{n+1} \quad (20)$$

<sup>247</sup> with corresponding observations

$$\eta_n = \mathbf{H}x_n + \sigma r_n \quad (21)$$

<sup>248</sup> where  $\mathbf{H} = [1 \ 0]$ ,  $\zeta_n = \mathbf{H}x_n$  and  $\rho \in \mathbb{R}^{D \times D}$  is the model error standard deviation. We assume  
<sup>249</sup> that the model and observations are corrupted by random noise. For these experiments we  
<sup>250</sup> have  $x_n \in \mathbb{R}^2$  and  $\eta_n \in \mathbb{R}$ . The model errors,  $q_n$ , are assumed to be serially independent  
<sup>251</sup> errors with mean  $\mathbb{E}q_n = 0$  and variance  $\mathbb{E}q_n q_n^T = \mathbb{I}$ .

<sup>252</sup> We set up an observer analogous to our sequential scheme (19),

$$z_{n+1} = \hat{z}_{n+1} + \mathbf{K}_n(\eta_{n+1} - \mathbf{H}\hat{z}_{n+1}), \quad y_n = \mathbf{H}z_n \quad (22)$$

<sup>253</sup> where

$$\hat{z}_{n+1} = \underbrace{\begin{bmatrix} -1 & 10 \\ 0 & 0.5 \end{bmatrix}}_{\mathbf{A}} z_n. \quad (23)$$

<sup>254</sup> In this case the model is coupled to the observations through a linear coupling term which  
<sup>255</sup> is dependent on the difference between the actual output and the expected output value  
<sup>256</sup> based on the next estimate of the state. For these experiments we will take the coupling  
<sup>257</sup> matrix  $\mathbf{K}_n$  to be constant so from here on we write  $\mathbf{K}_n = \mathbf{K}$ .

<sup>258</sup> The error dynamics in this linear example are given by

$$\begin{aligned} e_{n+1} &= x_{n+1} - z_{n+1} \\ &= (\mathbf{A} - \mathbf{K}\mathbf{H}\mathbf{A})e_n + \mathbf{K}r_{n+1} - (\mathbb{I} - \mathbf{K}\mathbf{H})q_{n+1}. \end{aligned} \quad (24)$$

<sup>259</sup> Since the noisy part of the error dynamics (Eq. 24) is stationary, synchronisation can  
<sup>260</sup> be guaranteed if the eigenvalues of the matrix  $(\mathbf{A} - \mathbf{K}\mathbf{H}\mathbf{A})$  all lie within the unit circle.  
<sup>261</sup> Synchronisation here means that the error dynamics is asymptotically stationary with finite  
<sup>262</sup> covariance. To achieve this, we use a result from control theory, for which we need a few  
<sup>263</sup> definitions. Let  $\mathbf{H}\mathbf{A} = \mathbf{C}$  so that the error dynamics are described by the system matrix  
<sup>264</sup>  $(\mathbf{A} - \mathbf{K}\mathbf{C})$ . A pair of matrices  $(\mathbf{A}, \mathbf{C})$  is called *observable* if the observability matrix

$$\mathcal{O} = [\mathbf{C} \ \mathbf{CA} \ \mathbf{CA}^2 \ \dots \ \mathbf{CA}^{D-1}]^T \quad (25)$$

<sup>265</sup> has full rank. If this condition holds then the poles of the matrix  $(\mathbf{A} - \mathbf{K}\mathbf{C})$  can be placed  
<sup>266</sup> anywhere in the complex plane by proper selection of  $\mathbf{K}$ . In particular they can be placed  
<sup>267</sup> within the unit circle<sup>19</sup>.

<sup>268</sup> In our example,  $x_n \in \mathbb{R}^2$  so our observability matrix is

$$\mathcal{O} = [\mathbf{H}\mathbf{A} \quad \mathbf{H}\mathbf{A}^2]^T. \quad (26)$$

<sup>269</sup> It is straightforward to check that the linear system we are working with here is observable  
<sup>270</sup> even though  $\mathbf{A}$  is not stable.

<sup>271</sup> It is well known in Kalman Filter theory (see for example Anderson and Moore<sup>20</sup>) that  
<sup>272</sup> the optimal gain matrix  $\kappa_n$  for a linear filter (in the sense of giving least error covariance) is  
<sup>273</sup> the Kalman Gain which is defined by

$$\kappa_n = \Sigma_n \mathbf{H}^T (\mathbf{H} \Sigma_n \mathbf{H}^T + \sigma^2)^{-1} \quad (27)$$

<sup>274</sup> where  $\Sigma_n$  is the error covariance matrix defined by  $\Sigma_n = \mathbb{E}[(\hat{z}_n - x_n)(\hat{z}_n - x_n)^T]$  and expressed  
<sup>275</sup> by the following recursive equation,

$$\Sigma_n = \mathbf{A}(\Sigma_n - \Sigma_n \mathbf{H}^T (\mathbf{H} \Sigma_n \mathbf{H}^T + \sigma^2)^{-1} \mathbf{H} \Sigma_n) \mathbf{A}^T + \rho^2 \cdot \mathbb{1}. \quad (28)$$

<sup>276</sup> Kalman Filter theory states that for  $n$  large, the error covariance  $\Sigma_n$  converges to  $\Sigma_\infty$  which  
<sup>277</sup> is the solution to

$$\Sigma_\infty = \mathbf{A}[\Sigma_\infty - \Sigma_\infty \mathbf{H}^T (\mathbf{H} \Sigma_\infty \mathbf{H}^T + \sigma^2)^{-1} \mathbf{H} \Sigma_\infty] \mathbf{A}^T + \rho^2 \cdot \mathbb{1}. \quad (29)$$

<sup>278</sup> This in turn implies that the Kalman Gain (27) converges to the asymptotic gain which is  
<sup>279</sup> defined by

$$\kappa_\infty = \Sigma_\infty \mathbf{H}^T (\mathbf{H} \Sigma_\infty \mathbf{H}^T + \mathbf{R})^{-1} \quad (30)$$

<sup>280</sup> The asymptotic gain,  $\kappa_\infty$ , is obtained by solving the Discrete Algebraic Riccati Equation  
<sup>281</sup> (DARE) given by (29) and using the solution to calculate (30). Using Maple's inbuilt DARE  
<sup>282</sup> solver we were able to find the solution to this equation for the experimental setup described  
<sup>283</sup> above. The Algebraic Riccati Equation is solved using the method described in Arnold III  
<sup>284</sup> and Laub<sup>21</sup>.

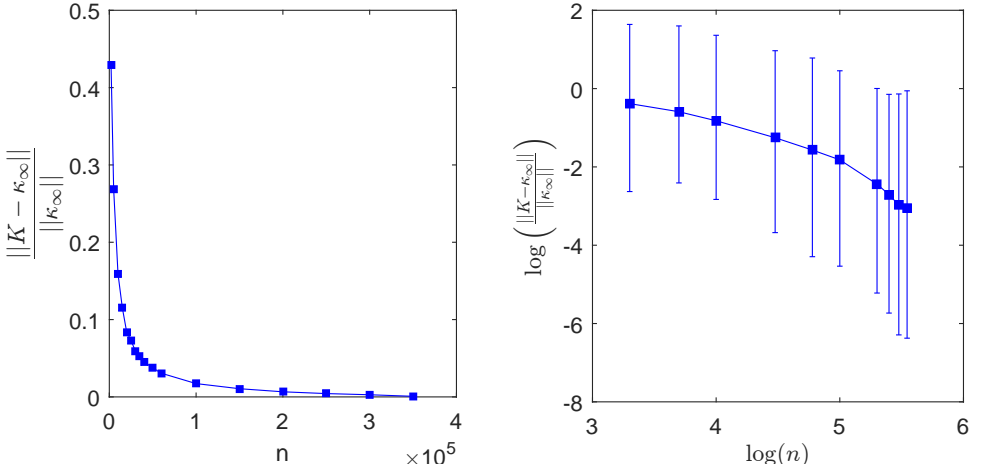
<sup>285</sup> The aim of this experiment is to estimate the optimal gain matrix,  $\kappa_\infty$  without referring  
<sup>286</sup> to the DARE, in particular without knowledge of  $\rho$ . We do this by minimising the empirical  
<sup>287</sup> out-of-sample error with respect to  $\mathbf{K}$ . In other words, our estimate of  $\kappa_\infty$  is the minimiser of  
<sup>288</sup>  $\hat{E}_O$  for a large (but finite) set of observations (paragraph a. below). This strategy is motivated  
<sup>289</sup> by our previous discussion about the out-of-sample error being an adequate measure of  
<sup>290</sup> performance. In fact, in the context of linear systems, we can prove (see Appendix A for

291 details) that the out-of-sample error is equivalent (in a certain sense) to the asymptotic  
 292 covariance of  $e_n$  as a measure of performance. We also stress that estimating the optimism  
 293 only requires knowledge of  $\mathbf{A}, \mathbf{H}, \sigma$  but not  $\rho$ , the model noise. This is the term that is  
 294 difficult to determine operationally, so estimating the optimism in an operational situation is  
 295 possible as all the required terms are readily available. In paragraph b. we discuss a variant  
 296 of this experiment where the gain matrix is supposed to be optimal under the constraint  
 297 that the characteristic polynomial has a certain shape.

298 *a. Estimating optimal gain matrix* The results obtained in this first experiment are  
 299 shown in Figure 1. The model noise is iid with  $\mathbb{E}q_n = 0$ ,  $\mathbb{E}q_n q_n^T = 1$  and  $\rho = 0.01$  while  
 300 for the observational noise, which was also iid with mean zero and variance one, we used  
 301  $\sigma = 0.1$ . We let  $n$  vary between zero and  $3.5 \times 10^5$ . For each  $n$  the empirical out-of-sample  
 302 error was minimised and the minimiser was recorded as an estimate of  $\kappa_\infty$ . The experiment  
 303 was repeated for 100 realisations of the observational noise,  $r_n$  so that the estimates were  
 304 different every time. As a measure of accuracy, 90% confidence intervals were constructed.  
 305 We expect that the estimates converge to the asymptotic gain  $\kappa_\infty$  given by the solution of  
 306 (29,30).

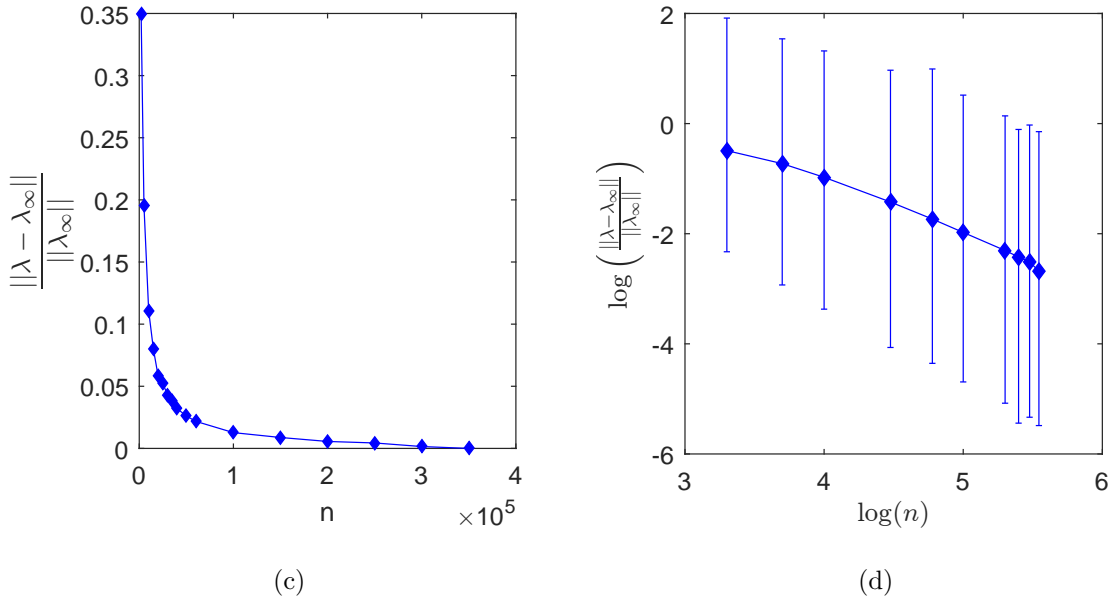
307 The results obtained are shown in Figure 1. Figure 1(a) shows a plot in blue squares  
 308 of the quantity  $\|\mathbf{K} - \kappa_\infty\| / \|\kappa_\infty\|$  against  $n$ . The figure shows that the gain matrix that  
 309 minimises the out-of-sample error converges exponentially to the asymptotic gain. Moreover,  
 310 it is illustrated in Figure 1(c) that the eigenvalues of the matrix  $(\mathbf{A} - \mathbf{K}\mathbf{H}\mathbf{A})$  for each gain  
 311 minimising the out-of-sample error, converge to the eigenvalues of the matrix  $(\mathbf{A} - \kappa_\infty \mathbf{H}\mathbf{A})$ .  
 312 Figure 1(c) shows the quantity  $\|\lambda - \lambda_\infty\| / \|\lambda_\infty\|$  against  $n$  in blue diamonds, where  $\lambda$   
 313 represents the eigenvalues of the matrix  $(\mathbf{A} - \mathbf{K}\mathbf{H}\mathbf{A})$ . The convergence of the eigenvalues is  
 314 also exponential. The values of these eigenvalues confirm that the minimising gains stabilise  
 315 the system since all of them are within the unit circle.

316 The remaining two figures in Figure 1 show a log plot of the same information outlined  
 317 above. Figure 1(b) represents the convergence of the gain matrices while Figure 1(d) shows  
 318 the same information for the eigenvalues. Both plots are almost straight lines as expected  
 319 since the convergence has already been noted to be exponential. The addition to these plots  
 320 are the 90% confidence intervals. As previously stated, the experiment was repeated for 100  
 321 realisations of the observational noise and the plotted confidence intervals represents the  
 322 uncertainty in the numerical experiment. The lower limit of the error bars was taken at the



(a)

(b)



(c)

(d)

FIG. 1. Figure 1(a) shows the convergence of the gain minimising the out-of-sample error to the asymptotic gain for increasing  $n$ . We plot the quantity  $\|\mathbf{K} - \kappa_\infty\| / \|\kappa_\infty\|$  against  $n$  in blue squares. Figure 1(b) shows a log plot of the same information with 90% confidence intervals. Figure 1(c) shows the quantity  $\|\lambda - \lambda_\infty\| / \|\lambda_\infty\|$  against  $n$  in blue diamonds, where  $\lambda = (\lambda_1, \lambda_2)$  represents the eigenvalues of the matrix  $(\mathbf{A} - \mathbf{KHA})$ . It is evident that the eigenvalues of the matrix  $(\mathbf{A} - \mathbf{KHA})$  for each gain minimising the out-of-sample error, converge to the eigenvalues of the matrix  $(\mathbf{A} - \kappa_\infty \mathbf{HA})$ , with  $n$  increasing. Figure 1(d) shows a log plot of the same information with 90% confidence intervals.

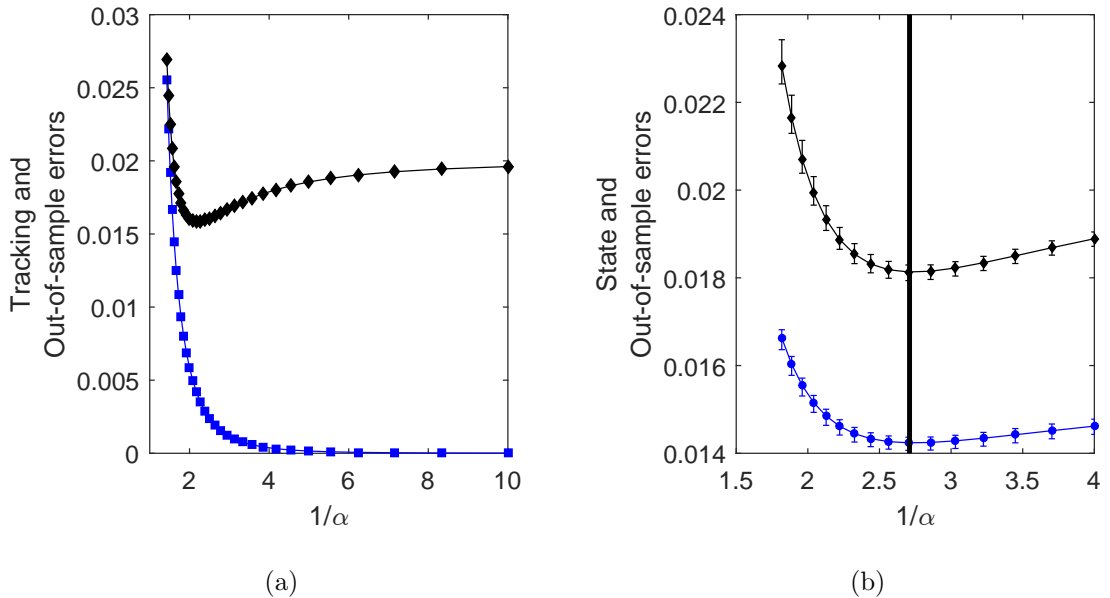


FIG. 2. Figure 2(a) shows a plot of the tracking error in blue squares and the out-of-sample error in black diamonds. The errors are plotted against the inverse of  $\alpha$  for  $\sigma = 0.1$  and  $\rho = 0.01$ . Figure 2(b) shows a plot of the out-of-sample error in black diamonds for 100 realisations of the noise  $r_n$  with  $\sigma = 0.1$  as well as the state error in blue circles. They are displayed for the range of  $\alpha$  where the minimum occurs. The error bars in both curves represent 90% confidence intervals. The black vertical line draws attention to the minimum of the out-of-sample error which coincides with the minimum of the state error.

<sup>323</sup> fifth percentile while the upper limit was taken at the 95th percentile thus creating the 90%  
<sup>324</sup> confidence intervals.

325      *b. Gain Matrix with Symmetric Poles*   In this part of the linear numerical experiment,  
 326 we want  $(\mathbf{A} - \mathbf{K}\mathbf{H}\mathbf{A})$  to have a certain characteristic polynomial. Suppose that the desired  
 327 characteristic equation is given by

$$q(\lambda) = (\lambda + \alpha)(\lambda - \alpha) \quad (31)$$

so that  $\lambda_1 = -\lambda_2$  and  $|\lambda_1| = |\lambda_2| = \alpha$ . The appropriate  $\mathbf{K}$  for a desired characteristic polynomial,  $q(\lambda)$  of the matrix  $(\mathbf{A} - \mathbf{K}\mathbf{H}\mathbf{A})$  follows from Ackermann's Formula<sup>19</sup> which is given by

$$\mathbf{K} = q(A)\mathcal{O}^{-1}[0 \dots 1]^T \quad (32)$$

331 where  $\mathcal{O}$  is the observability matrix defined in (26).

332 The results obtained from our numerical experiment to test the validity of (16) are shown  
 333 in Figure 2. Figure 2(a) shows a plot of the tracking error in blue squares and the out-of-  
 334 sample error in black diamonds. The out-of-sample error calculated via (16) is equivalent to  
 335 calculating the out-of-sample error explicitly using the output error. We can see that the  
 336 tracking error tends to zero with decreasing  $\alpha$ . This is what we expected and is confirmed  
 337 by using our analytical expression for the optimism.

338 It is clear from Figure 2(a) that while the tracking error tends to zero, the out-of-sample  
 339 error initially decreases and then increases resulting in a well-defined minimum. This is  
 340 because as the coupling strength increases, the observations are tracked too closely and thus  
 341 the output adapts too closely to the observations resulting in an increase of the out-of-sample  
 342 error. On the other hand when  $\alpha$  is large and the coupling strength is weak, the observations  
 343 are tracked poorly resulting in large tracking and out-of-sample errors. In these experiments  
 344  $\alpha$  was varied between 0 and 1 with the assimilation window taken to be  $N = 10000$ .

345 The well defined minimum of the out-of-sample error is also shown in Figure 2(b).  
 346 Figure 2(b) shows the out-of-sample error in black diamonds for the range of  $\alpha$  where  
 347 the minimum occurs. The figure shows the out-of-sample error for 100 realisations of the  
 348 observation noise  $r_n$  with  $\sigma = 0.1$  so that the sample estimate is different each time. The  
 349 error bars in the plot represent 90% confidence intervals for each value of  $\alpha$ . The lower  
 350 limit of the error bars is taken at the fifth percentile, while the upper limit is taken at the  
 351 95th percentile, hence obtained 90% confidence intervals as a measure of accuracy. Some  
 352 further experiments using different values of  $\sigma$  were carried out however the results are  
 353 not included here. The results produced were the same as the ones presented in this paper;  
 354 the only difference was the size of the error bars produced. A smaller value of  $\sigma$  resulted in  
 355 smaller error bars.

356 To quantify the variation of the parameter  $\alpha$  in this experiment, we considered the  
 357 following calculation. The mean value of the optimal  $\alpha$  plus/minus one standard deviation  
 358 in this case is

$$\bar{\alpha}^* \pm \sqrt{(\alpha^* - \bar{\alpha}^*)^2} = 0.3698 \pm 0.028. \quad (33)$$

359 The second plot in Figure 2(b) illustrates the state error. This estimate of the state error  
 360 is defined by

$$\hat{E}_S = \frac{1}{N} \sum_{n=1}^N (z_n - x_n)^2. \quad (34)$$

361 This is the error that ultimately wants to be analysed and minimised in data assimilation  
 362 experiments. However, because the model noise ( $\rho q_n$ ) is difficult to determine, we cannot  
 363 explicitly analyse the state error which is why we consider errors we can calculate, namely  
 364 the tracking, output or out-of-sample errors. We can plot the state error  $\hat{E}_S$  in this example  
 365 because we have access to it, however in general this is not possible. The vertical line in  
 366 Figure 2(b) draws attention to the minimum of the out-of-sample error. It is evident that the  
 367 state error also has a minimum and the plot suggests that the minima of the out-of-sample  
 368 and the state error are the same. Again, we ran the experiment for 100 realisations and  
 369 plotted the error bars with 90% confidence intervals.

## 370 B. Numerical Experiment 2: Hénon Map

371 In this experiment, the reality is given by

$$x_{n+1} = \underbrace{\begin{bmatrix} a & b \\ 1 & 0 \end{bmatrix}}_A x_n + c \begin{bmatrix} (\mathbf{H}x_n)^2 \\ 0 \end{bmatrix} + d \quad (35)$$

372 which for the values  $a = 0$ ,  $b = 0.3$ ,  $c = -1.4$ ,  $d = [1 \ 0]^T$  is the chaotic Hénon Map with  
 373 corresponding observations

$$\eta_n = \mathbf{H}x_n + \sigma r_n \quad (36)$$

374 where  $\mathbf{H} = [1 \ 0]$ , and  $\zeta_n = \mathbf{H}x_n$ . The model describing the reality is completely deterministic  
 375 and we assume that the observations are corrupted by random noise. Notice that we now  
 376 have a non linear term in the dynamical system. Such systems are said to be in Lur'e form.

377 Once again we consider data assimilation by means of synchronisation so we set up an  
 378 observer roughly analogous to our sequential scheme (19) with certain differences,

$$z_{n+1} = \hat{z}_{n+1} + \mathbf{K}_n(\eta_{n+1} - \mathbf{H}\hat{z}_{n+1}), \quad y_n = \mathbf{H}z_n \quad (37)$$

379 where

$$\hat{z}_{n+1} = \underbrace{\begin{bmatrix} a & b \\ 1 & 0 \end{bmatrix}}_A z_n + c \begin{bmatrix} \eta_n^2 \\ 0 \end{bmatrix} + d \quad (38)$$

380 where  $a, b, c, d$  are the same as for the reality. In this case as in the first example, the  
 381 model is coupled to the observations through a linear coupling term which is dependent on

382 the difference between the actual output and the output value expected based on the next  
 383 estimate of the state. However there is also a non linear coupling introduced here by the  
 384 presence of  $\eta_n^2$  in the background term. Note that (16) is still valid nonetheless because  $\hat{z}_{n+1}$   
 385 is still uncorrelated with  $r_{n+1}$ . For these experiments we will take the coupling matrix  $\mathbf{K}_n$  to  
 386 be constant so from here on in we write  $\mathbf{K}_n = \mathbf{K}$ .

387 We need to choose the matrix  $\mathbf{K}$  appropriately so that we can vary the coupling strength.  
 388 For illustration purposes consider the error dynamics for the noise-free situation so that  
 389  $\eta_n = \mathbf{H}x_n$ . The error dynamics in this case are given by

$$\begin{aligned}
 e_{n+1} &= x_{n+1} - z_{n+1} \\
 &= x_{n+1} - \hat{z}_{n+1} - \mathbf{K}\mathbf{H}(x_{n+1} - \hat{z}_{n+1}) \\
 &= (\mathbb{1} - \mathbf{K}\mathbf{H})(x_{n+1} - \hat{z}_{n+1}) \\
 &= (\mathbf{A} - \mathbf{K}\mathbf{H}\mathbf{A})(x_n - z_n) \\
 &= (\mathbf{A} - \mathbf{K}\mathbf{H}\mathbf{A})e_n.
 \end{aligned} \tag{39}$$

390 The matrix  $(\mathbf{A} - \mathbf{K}\mathbf{H}\mathbf{A})$  is stable even if  $\mathbf{K} = \mathbf{0}$ . This means that synchronisation occurs  
 391 even if there is no linear coupling between the model output and observations because of  
 392 the non linear coupling introduced in the model (38). The eigenvalues for such a case are  
 393  $\lambda_{1,2} = \pm\sqrt{b}$ , where  $b$  is as in the matrix  $\mathbf{A}$ . However, it might be that with noise, the  
 394 out-of-sample error is not optimal for this coupling and can be improved by some additional  
 395 linear coupling.

396 It is straightforward to check that the system we are working with here is observable  
 397 provided that  $b \neq 0$ . The appropriate  $\mathbf{K}$  for a desired characteristic polynomial,  $q(\lambda)$  of the  
 398 matrix  $(\mathbf{A} - \mathbf{K}\mathbf{H}\mathbf{A})$  again follows from Ackermann's Formula (32). Suppose that the desired  
 399 characteristic equation is given by

$$q(\lambda) = (\lambda + \alpha)(\lambda - \alpha) \tag{40}$$

400 so that  $\lambda_1 = -\lambda_2$  and  $|\lambda_1| = |\lambda_2| = \alpha$ . Then by Ackermann's formula we get

$$\mathbf{K} = \begin{bmatrix} 1 - \alpha^2/b \\ a\alpha^2/b^2 \end{bmatrix} \Rightarrow \mathbf{H}\mathbf{K} = 1 - \frac{\alpha^2}{b} \tag{41}$$

401 where  $a = 0$  and  $b = 0.3$  as in the matrix  $\mathbf{A}$ . From (41) we see that  $\mathbf{HK} = 1$  if  $\alpha = 0$ . Thus,

$$y_n = \mathbf{Hz}_n = (\mathbb{1} - \mathbf{HK})\mathbf{H}\hat{z}_n + \mathbf{HK}\eta_n \rightarrow \eta_n, \quad (42)$$

402 meaning that our data assimilation scheme simply replaces  $y_n$  with  $\eta_n$ , implying that the  
403 tracking error is zero. In other words, in this example, it is possible to render the eigenvalues  
404 of the error dynamics exactly zero and also to obtain zero tracking error. However, the data  
405 assimilation is not perfect and the out-of-sample and state errors will not necessarily be  
406 small.

407 Therefore, from (16) we know that

$$\hat{E}_O = \hat{E}_T - 2\sigma^2 \left( 1 - \frac{\alpha^2}{b} \right) - \sigma^2. \quad (43)$$

408 Recall that the aim of this work is to find a way to estimate the out-of-sample error to get a  
409 more realistic picture of model performance. We have already determined that when there  
410 is no linear coupling (i.e.  $\mathbf{K} = \mathbf{0}$ ) the system is stable and synchronisation occurs. We can  
411 see from (43) that this happens when  $\alpha = \pm\sqrt{b}$ . There are two further cases to consider.  
412 When  $\alpha^2 > b$  the feedback, due to the linear coupling, is negative. Therefore, in this case  
413 we will not be able to improve the out-of-sample error. However as  $\alpha$  tends to zero the  
414 optimism will increase and be bounded by  $2\sigma^2$ . Therefore when  $\alpha^2 < b$  it may be possible to  
415 improve the out-of-sample error and determine a coupling matrix  $\mathbf{K} \neq \mathbf{0}$ , that minimises the  
416 out-of-sample error, to be used in the model. We calculate the errors as we did for the linear  
417 numerical example in Section III A.

418 The results obtained from our numerical experiment to test the validity of (16) are shown  
419 in Figure 3. Figure 3(a) shows the tracking error in blue squares and the out-of-sample error  
420 in black diamonds. We can see that the tracking error tends to zero with decreasing  $\alpha$ . This  
421 is what we expected and is confirmed by using our analytical expression for the optimism.  
422 In these experiments  $\alpha$  was varied between 0 and 1 with the assimilation window taken to  
423 be  $N = 10000$ .

424 By analysing the expression for the optimism in this case, we see that there is a point  
425 where the tracking and out-of-sample errors meet. This happens when  $\alpha^2 = b$ . To the left of  
426 this, when  $\alpha^2 > b$ , the tracking error is greater than the out-of-sample error. To the right,  
427 when  $\alpha^2 < b$ , the tracking error is smaller than the out-of-sample error. In fact the tracking  
428 error tends to zero while the out-of-sample error decreases and then starts to increase again  
429 resulting in a well defined minimum.

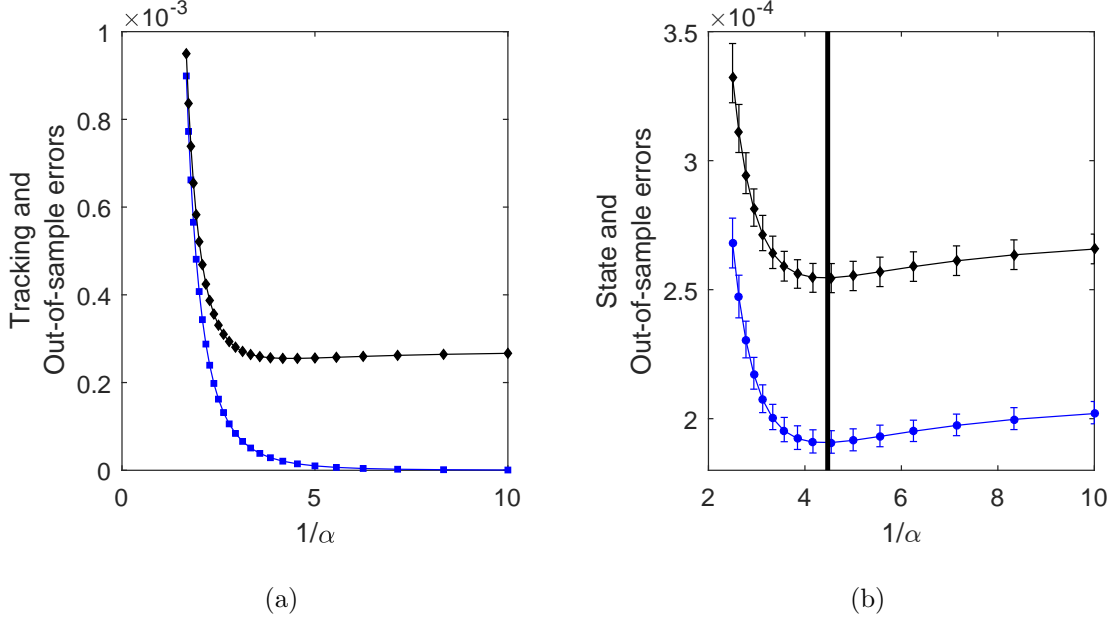


FIG. 3. Figure 3(a) shows a plot of the tracking error in blue squares and the out-of-sample error in black diamonds. The errors are plotted against the inverse of  $\alpha$  for  $\sigma = 0.01$ . Figure 3(b) shows a plot of the out-of-sample error in black diamonds for 100 realisations of the noise  $r_n$  with  $\sigma = 0.01$ . It is displayed for the range of  $\alpha$  where the minimum occurs. The error bars represent 90% confidence intervals. The state error is shown in blue circles also for 100 realisations of the observation noise with 90% confidence intervals. The vertical line draws attention to the minimum of both curves.

430 The well defined minimum of the out-of-sample error is shown more clearly in Figure 3(b).  
 431 Figure 3(b) shows the out-of-sample error in black diamonds for the range of  $\alpha$  where the  
 432 minimum occurs. The figure shows the out-of-sample error for 100 realisations of the noise  
 433  $r_n$  for  $\sigma = 0.01$ . The error bars represent 90% confidence intervals for each  $\alpha$ . Once again we  
 434 would like to quantify the variation of the parameter  $\alpha$ . The mean value of the optimal  $\alpha$   
 435 plus/minus one standard deviation in this case is

$$\bar{\alpha}^* \pm \sqrt{(\bar{\alpha}^* - \bar{\alpha}^*)^2} = 0.2238 \pm 0.0079. \quad (44)$$

436 Figure 3(b) also shows a plot of the state error in blue circles for 100 realisations. The  
 437 black, vertical line draws attention to the minimum of both curves. We can see that the  
 438 minimising gain is the same for both errors. When running data assimilation schemes, the  
 439 state error is the error we are interested in minimising, however we only have access to the  
 440 error in observation space. Even though this is the case, we have shown numerically that the

441 minimising gain is the same for both errors, even in this non linear situation.

442 As with the linear numerical experiment presented in Section III A, further experiments  
443 using different values of  $\sigma$  were carried out. The results produced were the same as the  
444 ones presented here; the only difference was the size of the error bars produced. A smaller  
445 value of  $\sigma$  resulted in smaller error bars much like it did for the linear numerical example.

446 What is particularly of interest here is that even though the dynamical system included  
447 a non linear term, the methodology still applies, provided that the matrix  $(\mathbf{A} - \mathbf{K}\mathbf{H}\mathbf{A})$  is  
448 stable. As an aside, the experiment suggests that the eigenvalues of the linear part of the  
449 error dynamics have to be  $< 1 - \epsilon$  with some small but non-zero  $\epsilon$  in order to stabilise the  
450 error dynamics.

### 451 C. Numerical Experiment 3: Lorenz '96

452 For this third numerical experiment, the reality is given by the Lorenz'96 model which is  
453 governed by the following equations

$$\dot{x}_i = -x_{i-1}(x_{i-2} - x_{i+1}) - x_i + F \quad (45)$$

454 and exhibits chaotic behaviour for  $F = 8$ . By integrating the above differential equation with  
455 a time step  $\delta = 1.5 \times 10^{-2}$ , we obtain a discrete model for our reality which we denote by

$$x_{n+1} = \Phi(x_n). \quad (46)$$

456 We take corresponding observations of the form

$$\eta_n = \mathbf{H}x_n + \sigma r_n \quad (47)$$

457 where  $\mathbf{H}$  is the observation operator and  $r_n$  is iid noise. We shall take the state dimension to  
458 be  $D = 12$ , the observation space to be  $d = 4$  and we define the observation operator so that  
459 we observe every third element of the state; that is  $(x_1, x_4, x_7, x_{10})$ . The system we construct  
460 here is fully non-linear with linear observations.

461 The assimilating model will use the Lorenz'96 model coupled to the observations through  
462 a simple linear coupling term, as done in the the previous numerical experiments. We set  
463 the coupling matrix  $\mathbf{K}$ , to be defined by

$$\mathbf{K} = \kappa \mathbf{H}^T \quad (48)$$

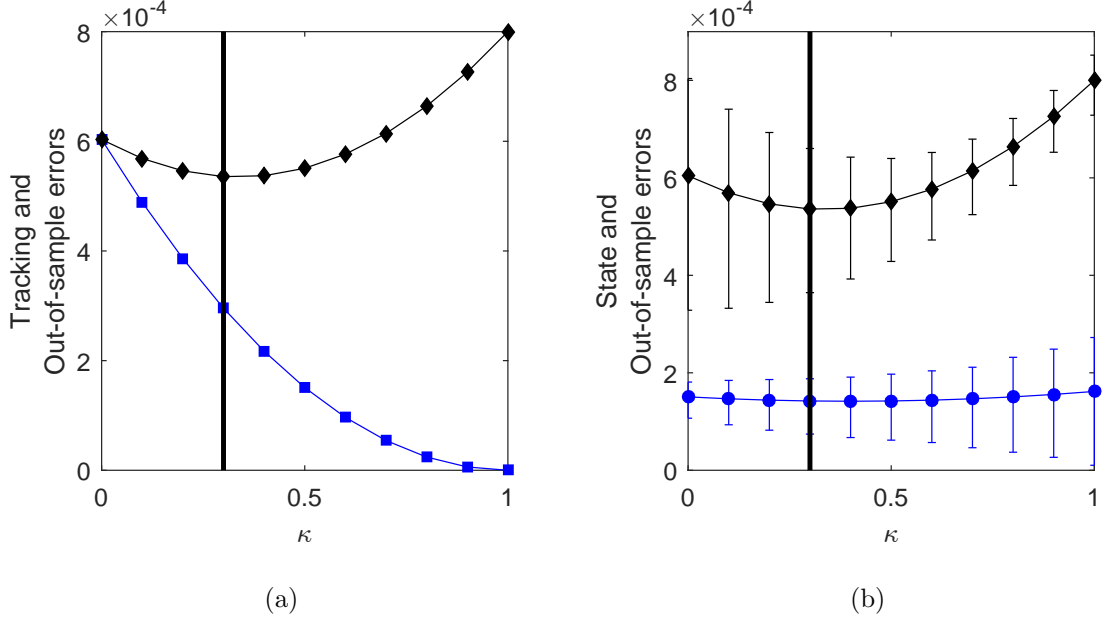


FIG. 4. Figure 4(a) presents the out-of-sample error (black diamonds) and the tracking error (blue squares). Figure 4(b) illustrates the out-of-sample error (black diamonds) and the state error (blue circles) with the error bars representing 90% confidence intervals. The black vertical line draws attention to the minimum of the out-of-sample error.

464 where  $\kappa$  is a coupling parameter taken to be between 0 and 1. With this information, the  
 465 assimilating model is defined by the following equations

$$\hat{z}_{n+1} = \Phi(z_n); \quad z_{n+1} = \hat{z}_{n+1} + \kappa \mathbf{H}^T (\eta_{n+1} - \mathbf{H} \hat{z}_{n+1}). \quad (49)$$

466 Once again we will vary the coupling strength in the observer by adjusting the coupling  
 467 parameter  $\kappa$ . If the coupling is too strong, the observations will be tracked too rigorously and  
 468 so the observational noise will not be filtered out. If the coupling is too weak the observations  
 469 are tracked poorly; so once again we expect the out-of-sample error to take a minimum at  
 470 some non-trivial value of  $\kappa$ .

471 As always we are interested in the behaviour of the state error and, ultimately, this is the  
 472 error we want to be minimal. We saw in Section III B that the minimiser for the out-of-sample  
 473 error was the same as for the state error. We investigate this here too.

474 The results obtained are shown in Figure 4. Once again the observational noise is iid with  
 475  $\mathbb{E} r_n = 0$ ,  $\mathbb{E} r_n r_n^T = 1$  and  $\sigma = 0.01$ . Since the gain is given by equation (48), the optimism  
 476 reduces to  $8\sigma^2\kappa$ . To see this note that the observation operator,  $\mathbf{H}$ , was defined so that  
 477 every third element of the state was observed. It follows then that  $\mathbf{H} \mathbf{H}^T = \mathbb{1}$ , the identity

478 matrix. Since we are observing four states, the trace of  $\mathbf{H}\mathbf{H}^T$  is equal to four. Thus, since  
 479 the optimism is defined by  $2\sigma^2\text{tr}(\mathbf{HK})$  and  $\mathbf{K}$  is given by equation (48), it follows that the  
 480 optimism reduces to  $8\sigma^2\kappa$ .

481 To calculate the the errors, a transient time was ignored to give the system time to  
 482 synchronise. In Figure 4(a) the out-of-sample error (black diamonds) is presented together  
 483 with the tracking error (blue squares). The black vertical line draws the eye to the minimum  
 484 of the out-of-sample error. As in the previous experiments, the tracking error reduces to zero  
 485 while the out-of-sample error increases eventually with increasing coupling strength.

486 Figure 4(b) presents the out-of-sample error (black diamonds) and the state error (blue  
 487 circles). The figure shows the errors for 100 realisations of the observational noise,  $r_n$ . The  
 488 error bars represent 90% confidence intervals for each value of  $\kappa$  with the lower limit of the  
 489 error bars taken at the fifth percentile and the upper limit taken at the 95th. The mean  
 490 value of the optimal  $\kappa$  plus/minus one standard deviation in this case is

$$\bar{\kappa}^* \pm \sqrt{(\kappa^* - \bar{\kappa}^*)^2} = 0.3050 \pm 0.1184. \quad (50)$$

491 The black line draws attention to the minimum of the out-of-sample error and we once  
 492 again see that the minima of the state and out-of-sample errors coincide. It is evident here  
 493 that these results support the results determined previously in the numerical experiments.  
 494 Further experiments using different values of  $\sigma$  where also carried out for this non linear  
 495 system. The results produced were the same as the ones presented here; the only difference  
 496 was the size of the error bars produced. Again, as with the results in the previous two  
 497 experiments, a smaller value of  $\sigma$  resulted in smaller error bars.

498 The flatness of the curves and the uncertainty shown in the figures are rather deceptive in  
 499 the plots presented in this paper. By looking at these figures, one might expect that the  
 500 errors in the estimate of  $\kappa^*$  are in fact quite large. However this is not the case as it is the  
 501 correlation between the errors in the plots that matters.

## 502 IV. CONCLUSIONS

503 A fundamental problem of data assimilation experiments in atmospheric contexts is that  
 504 there is no possibility of replication, that is, truly “out of sample” observations from the  
 505 same underlying flow pattern but with independent observational errors are typically not

506 available. A direct evaluation of assimilated trajectories against the available observations is  
507 likely to yield optimistic results though, since the observations were already used to find the  
508 solution.

509 A possible remedy was presented which simply consists of estimating that optimism,  
510 thereby giving a more realistic picture of the ‘out of sample’ performance. The optimism  
511 represents the correlation between the observations and the output of the data assimilation  
512 scheme. This estimate depends on the observational noise, the observation operator and the  
513 feedback gain matrix but not on the underlying dynamics or dynamical noise parameters.  
514 The model noise is the term that is difficult to determine operationally, so estimating the  
515 optimism in an operational situation is possible as all the required terms are readily available.  
516 In this paper, this approach was applied to data assimilation algorithms employing linear error  
517 feedback. Several numerical experiments concerning both linear and non-linear systems give  
518 evidence to the success of this method as it provides more realistic assessment of performance.  
519 This was demonstrated by comparing the out-of-sample performance with the true state  
520 error of the algorithm which was available in these numerical simulations.

521 The approach outlined above also provides a simple and efficient means to determine the  
522 optimal feedback gain by optimising the out-of-sample error with respect to the gain matrix.  
523 Further, theoretical results demonstrate that in linear systems with gaussian perturbations,  
524 the feedback thus determined will approach the optimal (Kalman) gain in the limit of large  
525 observational windows. The numerical experiments presented in this paper support this  
526 result for linear systems.

527 We cannot deduce the same thing for the non-linear systems since firstly, we do not have  
528 a candidate for the asymptotic error or gain since the Kalman Filter equations do not hold  
529 in these cases. Secondly, even if the existence of an optimal asymptotic gain could be proved,  
530 the sequence of minimisers might not converge to it.

531 As an outlook for future work, it seems that the presence of dynamical noise in the  
532 underlying system is important when considering the convergence of the optimal gain matrix  
533 for non-linear systems. (Even in the linear case, the presence of nondegenerate dynamical  
534 noise is essential for the proof to work). If there is no model noise present, then we cannot  
535 expect the gain matrix to converge in a meaningful way as the optimal asymptotic gain may  
536 not be well defined. For example it is possible that the dynamics of both the underlying  
537 system and model enter a region of stability, resulting in a reduction of the error. In this

538 case it would make sense to reduce or completely eliminate the feedback gain matrix. This  
 539 would need the gain matrix to be adaptive in some way; a concept not considered here.

540 **ACKNOWLEDGMENTS**

541 This paper was prepared with the support of the Engineering and Physical Sciences  
 542 Research Council for Jochen Bröcker under first grant agreement EP/L012669/1. The  
 543 authors wish to thank Peter Jan van Leeuwen for helpful discussions and constructive  
 544 suggestions which motivated some of the work in this paper.

545 **Appendix A**

546 In this appendix, we want to clarify the relationship between the output error

$$E_{O,n} = \mathbb{E}[(\mathbf{H}(x_n - z_n))^2] \quad (\text{A1})$$

547 (which we give an index  $n$  here as it depends on  $n$ ) and the error covariance matrix

$$\Gamma_n = \mathbb{E}[(x_n - z_n)(x_n - z_n)^T] \quad (\text{A2})$$

548 in the context of linear systems (Section III A). Re-writing the output error we obtain

$$\begin{aligned} E_{O,n} &= \mathbb{E}\{(\mathbf{H}(x_n - z_n))^T(\mathbf{H}(x_n - z_n))\} \\ &= \mathbb{E}\text{tr}\{(\mathbf{H}(x_n - z_n))^T\mathbf{H}(x_n - z_n)\} \\ &= \mathbb{E}\text{tr}\{\mathbf{H}(x_n - z_n)(x_n - z_n)^T\mathbf{H}^T\} \\ &= \text{tr}\{\mathbf{H}\Gamma_n\mathbf{H}^T\} \end{aligned} \quad (\text{A3})$$

549 and if we assume real values observations (i.e  $d = 1$ ), we get  $E_{O,n} = \mathbf{H}\Gamma_n\mathbf{H}^T$ . This does not  
 550 mean that  $E_{O,n}$  carries the same information as  $\Gamma_n$  since  $\mathbf{H}$  is not invertible.

551 To investigate this further, introduce the mappings  $F : \mathbb{R}^D \times \mathbb{R}^{D \times D} \rightarrow \mathbb{R}^{D \times D}$ ,  $(\mathbf{K}, \mathbf{M}) \rightarrow$   
 552  $(\mathbf{A} - \mathbf{K}\mathbf{H}\mathbf{A})\mathbf{M}(\mathbf{A} - \mathbf{K}\mathbf{H}\mathbf{A})^T$  and  $G : \mathbb{R}^D \rightarrow \mathbb{R}^{D \times D}$ ;  $\mathbf{K} \rightarrow \sigma^2\mathbf{K}\mathbf{K}^T + \rho^2(\mathbb{1} - \mathbf{K}\mathbf{H})(\mathbb{1} - \mathbf{K}\mathbf{H})^T$   
 553 and  $\Phi(\mathbf{K}, \mathbf{M}) = F(\mathbf{K}, \mathbf{M}) + G(\mathbf{K})$ . Note that  $F$  is linear in  $\mathbf{M}$ , and we will write  $F(\mathbf{K}) \cdot \mathbf{M}$   
 554 to emphasize this. It follows from linear filter theory that

$$\begin{aligned} \Gamma_{n+1} &= (\mathbf{A} - \mathbf{K}\mathbf{H}\mathbf{A})\Gamma_n(\mathbf{A} - \mathbf{K}\mathbf{H}\mathbf{A})^T + \sigma^2\mathbf{K}\mathbf{K}^T + \rho^2(\mathbb{1} - \mathbf{K}\mathbf{H})(\mathbb{1} - \mathbf{K}\mathbf{H})^T \\ &= F(\mathbf{K}) \cdot \Gamma_n + G(\mathbf{K}) = \Phi(\mathbf{K}, \Gamma_n). \end{aligned} \quad (\text{A4})$$

555 Suppose that  $\mathbf{K}$  is stabilising, then  $\Gamma_n \rightarrow \Gamma(\mathbf{K})$  which is a fixed point of (A4), i.e  $\Gamma(\mathbf{K}) =$   
556  $F(\mathbf{K}) \cdot \Gamma(\mathbf{K}) + G(\mathbf{K})$ . Note that  $\Gamma(\mathbf{K})$  describes the asymptotic error performance of the  
557 feedback  $\mathbf{K}$ .

558 We will now show that the output error is able to distinguish (asymptotically) between  
559 better and worse feedbacks. For any two symmetric matrices  $\mathbf{M}_1, \mathbf{M}_2$ , we write  $\mathbf{M}_1 \geq \mathbf{M}_2$  if  
560  $\mathbf{M}_1 - \mathbf{M}_2$  is positive semi-definite but not zero. Let  $\mathbf{K}_1, \mathbf{K}_2$  be two stabilising feedbacks so that  
561  $\Gamma(\mathbf{K}_1) \geq \Gamma(\mathbf{K}_2)$ ; that is  $\mathbf{K}_2$  performs better than  $\mathbf{K}_1$ . Further, assume  $(\mathbf{1} - \mathbf{H}\mathbf{K}_1) \neq 0$  which  
562 implies that  $(\mathbf{A} - \mathbf{K}_1\mathbf{H}\mathbf{A}, \mathbf{H})$  is observable. (This condition might seem artificial but we will  
563 see later that it is in fact rather natural). We will now show that  $\mathbf{H}\Gamma(\mathbf{K}_1)\mathbf{H}^T > \mathbf{H}\Gamma(\mathbf{K}_2)\mathbf{H}^T$ .  
564 Note that because  $\Gamma(\mathbf{K}_1) \geq \Gamma(\mathbf{K}_2)$  we have

$$\mathbf{M}_n = F^n(\mathbf{K}_1)\{\Gamma(\mathbf{K}_1) - \Gamma(\mathbf{K}_2)\} \geq 0 \quad (\text{A5})$$

565 for any  $n$  since  $F(\mathbf{K}_1)$  preserves positive and negative semi-definiteness. Further, the sequence  
566  $\mathbf{M}_n$  is decreasing. To see this, note that it must be monotone since

$$\mathbf{M}_{n+1} - \mathbf{M}_n = F(\mathbf{K}_1)\{\mathbf{M}_n - \mathbf{M}_{n-1}\} \quad (\text{A6})$$

567 and again  $F(\mathbf{K}_1)$  preserves definiteness. It cannot be increasing though since  $\mathbf{K}_1$  is stabilising  
568 and hence  $\mathbf{M}_n \rightarrow 0$ . Therefore  $\mathbf{H}\mathbf{M}_n\mathbf{H}^T \geq 0$  and decreasing.

569 Assuming  $\mathbf{H}\Gamma(\mathbf{K}_1)\mathbf{H}^T = \mathbf{H}\Gamma(\mathbf{K}_2)\mathbf{H}^T$  would then imply

$$\begin{aligned} 0 &= \mathbf{H}\mathbf{M}_n\mathbf{H}^T = \mathbf{H}F^n(\mathbf{K}_1)\{\Gamma(\mathbf{K}_1) - \Gamma(\mathbf{K}_2)\}\mathbf{H}^T \\ &= \mathbf{H}(\mathbf{A} - \mathbf{K}_1\mathbf{H}\mathbf{A})^n(\Gamma(\mathbf{K}_1) - \Gamma(\mathbf{K}_2))(\mathbf{A} - \mathbf{K}_1\mathbf{H}\mathbf{A})^{nT}\mathbf{H}^T \end{aligned} \quad (\text{A7})$$

570 for all  $n$ . Now using the spectral decomposition of  $\mathbf{M}_0 = \Gamma(\mathbf{K}_1) - \Gamma(\mathbf{K}_2)$ ,

$$\mathbf{M}_0 = \sum_{i=1}^d \lambda_i v_i v_i^T \quad (\text{A8})$$

571 where  $\lambda_i$  are the eigenvalues of  $\mathbf{M}_0$  and  $v_i$  are the corresponding eigenvectors, we see that

$$0 = \mathbf{H}\mathbf{M}_0\mathbf{H}^T = \sum_{i=1}^d \lambda_i (\mathbf{H}(\mathbf{A} - \mathbf{K}_1\mathbf{H}\mathbf{A})^n v_i)^2 \quad (\text{A9})$$

572 for all  $n$ . Since  $\mathbf{M}_0 \neq 0$ , there is a  $\lambda_j > 0$  and hence

$$\mathbf{H}(\mathbf{A} - \mathbf{K}_1\mathbf{H}\mathbf{A})^n v_j = 0 \quad \forall n \quad (\text{A10})$$

573 which contradicts the observability of  $(\mathbf{H}, \mathbf{A} - \mathbf{K}_1 \mathbf{H} \mathbf{A})$ . This shows that  $\mathbf{M}_0 = 0$  finishing  
 574 the proof.

575 From the preceding arguments, it follows that any minimiser of the output error must be  
 576 the asymptotic Kalman gain. To see this, assume  $\mathbf{K}_2$  is the Kalman gain while  $\mathbf{K}_1$  optimises  
 577 the output error  $\mathbf{H}\Gamma(\mathbf{K})\mathbf{H}^T$ . By definition of the kalman gain,  $\Gamma(\mathbf{K}_1) \geq \Gamma(\mathbf{K}_2)$ , and the  
 578 preceding discussion shows that  $\Gamma(\mathbf{K}_1) = \Gamma(\mathbf{K}_2)$  if  $(\mathbb{1} - \mathbf{H}\mathbf{K}_1) \neq 0$ .

579 To check that this is true, use that the asymptotic output error satisfies

$$\mathbf{H}\Gamma(\mathbf{K})\mathbf{H}^T = (\mathbb{1} - \mathbf{H}\mathbf{K})^2 \{ \mathbf{H}\Gamma(\mathbf{K})\mathbf{H}^T + \rho^2 \mathbf{H}\mathbf{H}^T \} + \sigma^2 (\mathbf{H}\mathbf{K})^2. \quad (\text{A11})$$

580 Taking the derivative with respect to  $\mathbf{K}$  at  $\mathbf{K}_1$  and using the optimality yields the condition

$$\mathbf{H}\mathbf{K}_1 = \frac{\mathbf{H}\Gamma(\mathbf{K}_1)\mathbf{H}^T + \mathbf{H}\mathbf{H}^T \rho^2}{\mathbf{H}\Gamma(\mathbf{K}_1)\mathbf{H}^T + \mathbf{H}\mathbf{H}^T \rho^2 + \sigma^2} \quad (\text{A12})$$

581 so  $\mathbb{1} = \mathbf{H}\mathbf{K}_1 > 0$ . As a final remark,  $\mathbb{1} - \mathbf{H}\mathbf{K} = 0$  implies that  $y_n = \eta_n$  (check example (22)  
 582 for constant  $\mathbf{K}$ ), that is the data assimilation simply reports back the observations.

## 583 REFERENCES

584 <sup>1</sup>C. M. Bishop, *Neural Networks for Pattern Recognition* (Oxford University Press Inc.,  
 585 1995).

586 <sup>2</sup>B. Efron, “How biased is the apparent error rate of a prediction rule?” Journal of the  
 587 American Statistical Association **81**, 461–470 (1986).

588 <sup>3</sup>T. Hastie, R. Tibshirani, and J. Friedman, *The Elements of Statistical Learning: Data  
 589 Mining, Inference and Prediction (Second Edition)* (Springer-Verlag, 2009).

590 <sup>4</sup>B. Efron, “The estimation of prediction error: Covariance penalties and cross-validation,”  
 591 Journal of the American Statistical Association **99** (2004).

592 <sup>5</sup>E. Kalnay, *Atmospheric Modeling, Data Assimilation and Predictability*, 1st ed. (Cambridge  
 593 University Press, 2001).

594 <sup>6</sup>G. Wahba, D. R. Johnson, F. Gao, and J. Gong, “Adaptive tuning of numerical weather  
 595 prediction models: Randomized GCV in three- and Four-Dimensional data assimilation,”  
 596 Monthly Weather Review (1995).

597 <sup>7</sup>G. P. Cressman, “An operational objective analysis system,” Monthly Weather Review **87**,  
 598 367–374 (1959).

599 <sup>8</sup>S. L. Barnes, "A technique for maximizing details in numerical weather map analysis,"  
600 Journal of Applied Meteorology **3**, 396–409 (1964).

601 <sup>9</sup>W. Lahoz, B. Khattatov, and R. Menard, *Data Assimilation: Making Sense of Observations*  
602 (Springer-Verlag, 2010).

603 <sup>10</sup>Y. Sasaki, "Some basic formalisms in numerical variational analysis," Monthly Weather  
604 Review **98**, 875–883 (1970).

605 <sup>11</sup>A. Lorenc, "A global three-dimensional multivariate statistical interpolation scheme,"  
606 Monthly Weather Review **109**, 701–721 (1981).

607 <sup>12</sup>A. H. Jazwinski, *Stochastic Processes and Filtering Theory Volume 64* (Academic Press  
608 Inc., 1970).

609 <sup>13</sup>A. Pikovsky, M. Rosenblum, and J. Kurths, *Synchronization: A Univeral Concept in*  
610 *Nonlinear Sciences* (Cambridge University Press, 2001).

611 <sup>14</sup>H. J. C. Huijberts, H. Nijmeijer, and A. Y. Pogromsky, "Discrete-time observers and  
612 synchronization," Controlling chaos and bifurcations in engineering systems , 439–455  
613 (1999).

614 <sup>15</sup>S. Boccaletti, J. Kurths, G. Osipov, D. Valladares, and C. Zhou, "The synchronization of  
615 chaotic systems," Physics Reports **366**, 1–101 (2002).

616 <sup>16</sup>J. Bröcker and I. G. Szendro, "Sensitivity and Out-Of-Sample Error in Continuous Time  
617 Data Assimilation," Quarterly Journal of the Royal Meteorological Society **138**, 1785–801  
618 (2012).

619 <sup>17</sup>I. G. Szendro, M. A. Rodríguez, and J. M. Lopez, "On the problem of data assimilation  
620 by means of synchronization," Journal Of Geophysical Research **114**, D20109 (2009).

621 <sup>18</sup>S.-C. Yang, D. Baker, and H. Li, "Data Assimilation as Synchronization of Truth and  
622 Model: Experiments with the Three-Variable Lorenz System," Journal of the Atmospheric  
623 Sciences **63**, 2340–2354 (2006).

624 <sup>19</sup>R. Dorf and R. Bishop, *Modern Control Systems Tenth Edition* (Pearson Education Inc.,  
625 2005).

626 <sup>20</sup>B. Anderson and J. Moore, *Optimal Filtering* (Dover Publications Inc, 1979).

627 <sup>21</sup>W. F. Arnold III and A. J. Laub, "Generalized eigenproblem algorithms and software for  
628 algebraic riccati equations," Proceedings of the IEEE **72**, 1746–1754 (1984).